Clearance and design optimization of bio-inspired bearings under off-center load

Delphine Sysaykeo, Emmanuel Mermoz, Thomas Thouveny

▶ **To cite this version:**

Delphine Sysaykeo, Emmanuel Mermoz, Thomas Thouveny. Clearance and design optimization of bio-inspired bearings under off-center load. CIRP Annals - Manufacturing Technology, 2020, 69 (1), pp.121-124. 10.1016/j.cirp.2020.03.006 . hal-03178702

HAL Id: hal-03178702
https://hal.science/hal-03178702v1

Submitted on 18 Jul 2022

HAL is a multi-disciplinary open access archive for the deposit and dissemination of scientific research documents, whether they are published or not. The documents may come from teaching and research institutions in France or abroad, or from public or private research centers.

L'archive ouverte pluridisciplinaire **HAL**, est destinée au dépôt et à la diffusion de documents scientifiques de niveau recherche, publiés ou non, émanant des établissements d'enseignement et de recherche français ou étrangers, des laboratoires publics ou privés.

Distributed under a Creative Commons Attribution - NonCommercial 4.0 International License

Version of Record: https://www.sciencedirect.com/science/article/pii/S0007850620300068
Manuscript_5b72339c45084b7656b5058ee48c537f

Contents lists available at SciVerse ScienceDirect

CIRP Annals Manufacturing Technology

Journal homepage: www.elsevier.com/locate/cirp

Clearance and design optimization of bio-inspired bearings under off-center load

Delphine Sysaykeo[a,b], Emmanuel Mermoz (2) [a,b], Thomas Thouveny [a]

[a] *Aix Marseille Univ, CNRS, ISM, Marseille, France*

[b] *Airbus Helicopters, Aéroport de Marseille Provence, Marignane, 13700 France*

Wear due to over-pressure is a well-known phenomenon that appears on bush bearing under off-center load. In this context, this paper proposes a methodology to develop a new bearing inspired from a lamb elbow. This bio-inspired bearing could replace bush bearing from helicopter's system. The method starts with the analysis of the contact surfaces of the biological joint from 3D scans. That allowed to extract a revolute profile for the bio-inspired bearing. Finite element simulations were then realized to find the best clearance specification to reduce contact pressure. The bio-inspired bearing is after optimized using Design Of Experiments method.

Biologically inspired design, Finite element method (FEM), Design optimization

1. Introduction

Misalignment of cylindrical joint is a frequent issue encountered in mechanical systems [1]. This can be due to part deformation, asymmetric loading and manufacturing errors [2]. The consequences are vibrations, wear and a lifespan reduction. Usually, when misalignment appears, the contact between the shaft and the outer ring is located near edges in a very restricted zone which leads to overpressure. In order to reduce wear in cylindrical bush bearings, a tight clearance could be applied. However, this requires small tolerance values and therefore an expensive machining. Design improvements can be found in literature [3] but none of the recent studies succeeded in reducing efficiently this over-pressure. Bio-inspiration in industry is a research path that could be useful to overcome this kind of issues when the classical mechanical technologies reach their limits [4]. The analysis of biological joint provides new design possibilities to propose innovative mechanical joint design [5]. For example, the profile of biological joint is composed of continuous and differentiable curves (see Humerus on Fig. 1a) whereas the mechanical technologies contain sharp angle and standard contact geometries like cylinders (Fig 1b). The topic of this paper is a methodology to design a bio-inspired bearing to replace bush bearing in industrial mechanism. To illustrate, the bio-inspired bearing could replace the bush bearings from the helicopter flight control system (Fig. 1b). In certain configuration, the pivot underwent asymmetric loads. These lead to overpressure on the part's endpoint and reduce the service life. To solve this problem, the lamb elbow joint was the source of inspiration. The lamb is part of unguligrade quadruped animal which undergo high mechanical stresses compare to bipeds [6]. The lamb is an animal easy to retrieve to study. Its elbow is kinematically comparable to a pivot link [6] [7]. Moreover, off-center loads are applied on its forelimb joints (yellow arrow in Fig. 1a). Thus, the observed joint forms are asymmetric (humerus in Fig 1a). A new methodology was proposed to design and optimize bio-inspired mechanical link for off-center load.

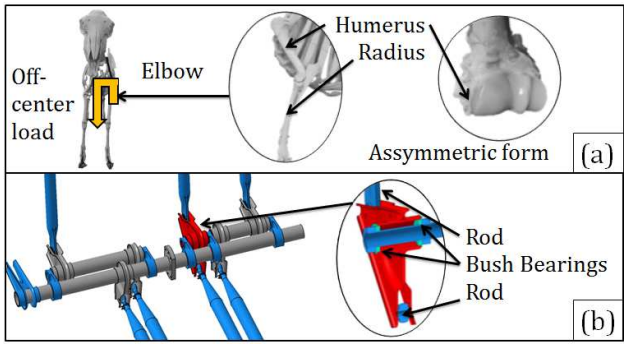

Figure 1. (a) Focus on lamb elbow.
(b) Focus on bush bearing from helicopter's flight control system.

2. Proposed bio-inspired joint design methodology

This methodology is articulated in four major phases:

- Contact zone measurements of the biological elbow joint: the surfaces of humerus/radius interfaces were digitalized with a 3D scan.
- Design of bio-inspired mechanical link: the contact zones were identified and humerus/radius profiles were selected. Bio-inspired profiles were retrieved and smoothed to design the new bio-inspired bearing.
- Choice of clearance specification: four different specifications to define the clearance topology were proposed. They were tested via Finite Elements Method (FEM) in order to obtain the optimal pressure distribution through off-center load.
- Optimization of the bio-inspired shape to reduce contact pressure via FEM: a first global Design of Experiments (DOE) was realized to evaluate which factors influence most the contact pressure distribution. Finally, a second local DOE was achieved using the two most influencing factors to find an optimum of contact pressure.

© 2020 published by Elsevier. This manuscript is made available under the CC BY NC user license
https://creativecommons.org/licenses/by-nc/4.0/

3. Geometrical bio-inspiration of bush bearings

3.1. Study of the interface surfaces of lamb elbow

In the literature, geometrical acquisition of bone structure is usually made by magnetic resonance imaging (MRI) or computed tomography (CT) [7]. These techniques typically offer a resolution of 0.5 and 0.1 mm, respectively. In contact mechanics, the accuracy of the geometry is critical on the pressure computation. Thus, an optical scanner GOM ATOS with a resolution of 0.02 mm was used in this study. In this work, an anatomical specimen was used. The lamb joint contact surfaces are localized in articular capsules. In consequence, the cartilage interfaces can't be measured directly by the optical scanner. The steps to bypass this problem are described as follows. Firstly, the complete fresh elbow was scanned, in a standing position, non-dismembered, with markers (like in Fig. 2a in [6]) fixed on each cortical bones. These markers will allow to know the relative position between the two bones. Secondly, the biological joint was dismembered and the two bones cartilages were scanned separately with their markers. The bone scans were made on a fresh elbow with an intact cartilage. Indeed, the cartilage is composed primarily of water (80%) and dries with time when bones are out of body. The cartilage has not a constant thickness on the elbow bone and is not proportional to the bone size [8]. This methodology is more accurate than working with dry bone. Thirdly, the humerus and radius scans were superposed to the complete specimen scan in Catia V5 using the markers. This way, the cartilages were in the biological position. Finally, the humerus and radius scans were numerically cleaned to remove the remaining fresh tissues (muscles, ligaments and synovial membrane). Thus, only the potential contact surfaces were kept. These surfaces have been colored assuming the different zones of potential contact (Fig. 2a and Fig. 2b).

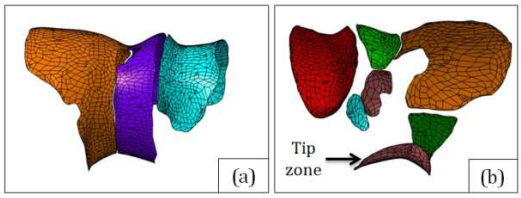

Figure 2. The humerus (a) and radius (b) cartilage surfaces resulting from 3D scan.

The humerus had three potential zones of contact whereas the radius had a larger number of zones. Thus the radius was more complex to analyze. Its zones involved in the contact with the humerus depend of the angular position of the forelimb. For example, the tip zone (in Fig. 2b) is involved when the elbow is in full extension and locked. In contrary, the humerus cartilage was easier to study. It was assimilated to a revolution surface. This assumption was validated after calculation of its axis by least squares (LSQ).

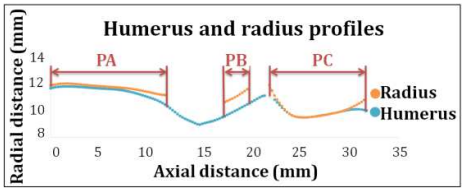

Figure 3. The selected profiles for 3 contact zones.

After that, humerus and radius profiles were generated from the intersection of a plan passing through the humerus axis with the cartilage surfaces. Thus, the contact zone between the humerus and radius can be observed. In a specific angular position of profiles, two contact zones were selected: PA and PC in Fig. 3. In these zones, the humerus and radius profiles were conforming. In this angular position, the third zone PB was also selected even if no contact was observed between the humerus and radius profiles. A contact could appear under axial load or with higher loadings.

3.2. Mechanical bio-inspiration link design

The bio-inspired bearing was designed by revolution of a smoothed humerus biological profile. Previous works have simplified the profile of human elbow by a series of lines and circular arcs [9]. In this study, the profile was smoothed with polynomials to best fit the biological profile. The curves from polynomials of degree higher than 2 give sweeping curves due to change of sign of their derivative. When these kinds of curve are in contact, overpressure could appear. Thus, each contact zones (PA, PB and PC) was smoothed with a polynomial of degree 2. The 3 polynomials were defined in local reference frame. Fig. 4 shows their equations with their coefficients. Theses coefficients will be used in the section 3. In our case study, the bearing was undergoing essentially off-center load. The axial load was low and supported principally by PB zone. The overall shape of the bio-inspired bearing has been designed following the smoothed humerus profile (Fig. 4). However, the clearance definition has also a huge impact on the bearing performance for complex shape and it will be study in the next paragraph.

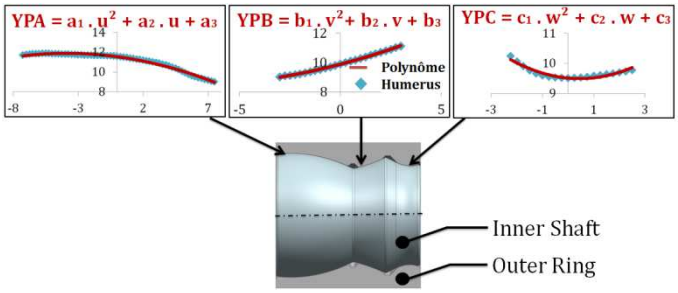

Figure 4. A bio-inspired bearing based on the 3 polynomials.

3.3. Clearance specification set for the bio-inspired bush bearing

Studies were already done on clearance specification and showed that a small dimensional change could improve the pressure distribution [10]. The aim of this section was to study the influence of four different clearance specifications for the bio-inspired bearing in term of contact pressure.

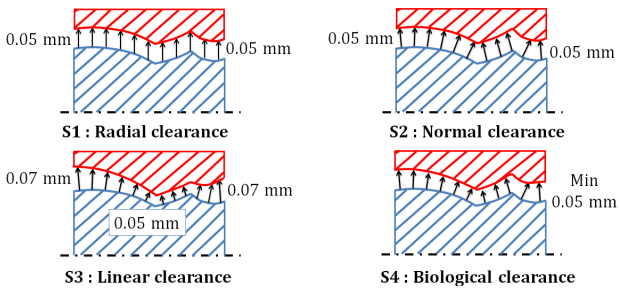

Figure 5. Set of clearance specifications.

The radial (S1 in Fig. 5) and normal (S2 in Fig. 5) clearance specifications are found in classical mechanical design. Thus, they were selected to be tested. In each specification, the inner shafts

were obtained by revolution of the smoothed humerus profile. In the radial clearance specification, the outer ring was a shaft profile offset of 0.05 mm in radial direction. The normal clearance specification had the same construction but in normal profile direction. The linear clearance specification (S3 in Fig. 5) allows to have a bigger gap at part edge. The over-pressure found under off-center load should thus decrease. The gap between the outer ring and the inner shaft was 0.05 mm in the middle part and 0.07 mm at the part edges with a linear law. Finally, the biological clearance specification (S4 in Fig. 5) was obtained by elbow interface observation. The outer ring was designed using a smoothed radius profile. It was smoothed by 3 polynomials of degree 2 like the inner shaft. This smoothed profile was translated in radial direction in order to have a minimum gap of 0.05 mm. For all the specifications, the minimum clearance was 0.1 mm diametrically. This corresponds to the clearance of the bush bearings from the helicopter flight control system (H8e9) which was a classical tolerance in bearing design.

3.4. Choice of the best clearance specification

To compare the set of clearance specifications, finite element simulations were realized with Simcenter (pre and post-processing) and Samcef mecano (solver) using the non-linear quasi-static module. The different bearings were tested for centered load (row C in Fig. 6) and off-center load in left side (row L_1 and L_2). L_1 is the bottom view and L_2 is the top view. The load of 500 N was applied to the shaft with an offset of 28 mm from the center via 1D rigid body element. The outer ring was embedded. The different bearings were meshed with hexahedral elements of degree 2. The edge size mesh was 0.2 mm for contact zone. The bearing materials were steel (E= 210 000 MPa and Poisson ratio= 0.3). The maximal contact pressure is indicated for each case in Fig. 6.

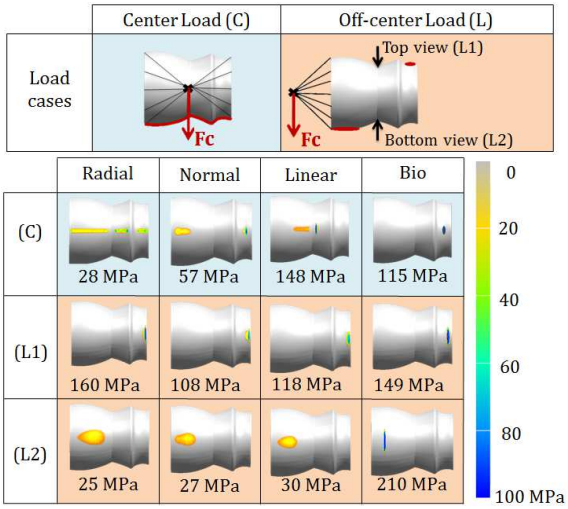

Figure 6. FEM results for clearance specification set.

Biological clearance specification was less efficient for all load cases. Their profiles were not as conforming as the other solutions and induced high contact pressure. One explanation was that a clearance was added between the smoothed humerus and radius profiles whereas there is actually no gap in cartilaginous joint. The humerus and radius cartilages are fully in contact in reality. The cartilage has indeed the capacity to be deformed under compressive load. On the contrary, the materials used in the FEM model have higher hardness than cartilage. The Young's modulus is 10 MPa for cartilage versus 210 000 MPa for steel. The radial clearance solution provided good pressure distribution for centered load but not for off-center load. In the opposite, linear clearance solution had high pressure for centered load and quite good result for off-center load. The trade off to obtain suitable behavior for centered and off-center loads was the normal clearance specification. Nevertheless, for all the clearance specifications, an over-pressure was observed in the right side of the top view since the contact zone was located too close to the edge of the bearing.

4. Bio-inspired shape optimization

In this section, the aim was to enhance the distribution of the contact pressure for off-center load. A first Design Of Experiment was realized to predict which parameters were the most influencing the pressure distribution. This first DOE surrogate model also allows to represent the solution design space to a large extent of parameters. Then, a second DOE surrogate model was defined with the two most influencing parameters to predict the local optimum in term of pressure distribution.

4.1. Design Of Experiments: First model

Five design parameters were used as DOE's factors (Table 1): a_1, a_2, c_1, c_2 (from Fig 4) and the *clearance*. The coefficient a_1 and c_1 are corresponding to the polynomial's curvature and a_2 and c_2 to the polynomial's slope. The coefficients a_3 and c_3 are related to the size of the bearing. They are design constraints in consequence they were fixed in this optimization study. The coefficients b_1, b_2 and b_3 (from Fig 4) are corresponding to the PB zone which was not a contact zone in the case of off-center load. So they were not used in this optimization. The DOE was following a Box-Behnken matrix. The sampling per factor was 3 and induced 41 FEM simulations. The Nominal values (Table 1) were the coefficients values of the best-fitted polynomials on the biological specimen. The variation values (Table 1) were calculated at ± 10 % of the nominal values. This describes the extension of research domain. The maximal contact pressure (Y_1) was chosen as the DOE's response. The Response Surface (RS) was defined with a polynomial of degree 2 and had 21 coefficients (Eq.1). Where L_i and $L_{i,j}$ were the response surface coefficients, X_i were the normalized values of P_i (Eq.2) and P_i were the factor values.

$$Y_1 = L_0 + L_1.X_1 + \dots + L_5.X_5 + L_{12}.X_1.X_2 + \dots + L_{45}.X_4.X_5 + L_{11}.X_1^2 + \dots + L_{55}.X_5^2 \quad (1)$$

$$X_i = \frac{P_i - Nominal}{Variation} \quad (2)$$

Table 1
DOE parameters and results of the first model.

	Factor	Nominal	Variation	Opt. Val.	Partial Deriv.
P_1	a_1	0.0225	0.00225	0.02045	66.37
P_2	a_2	0.1754	0.01754	0.17532	0.30
P_3	c_1	0.0874	0.00874	0.09093	-29.52
P_4	c_2	0.0783	0.00783	0.07841	-1.11
P_5	*clearance*	0.1	0.01	0.09917	6.01

L_i and $L_{i,j}$ coefficients were calculated thanks to the FEM results using LSQ method. The factor values (P_i) to minimize the maximum contact pressure was found in Optimum values column. The partial derivatives of the five factors were calculated to determine their local effect. Equation 3 shows an example of this calculation for the partial derivative respect to X_1.

$$\frac{\partial Y_1}{\partial X_1} = L_1 + L_{12}.X_2 + L_{13}.X_3 + L_{14}.X_4 + L_{15}.X_5 + 2.L_{11}.X_1 \quad (3)$$

The factors a_1 and c_1 had the largest partial derivative in absolute value (in blue in Partial Deriv. column). They have thus the greatest influence on the contact pressure around the optimum point. That means a little change of the curvature value increases the maximum contact pressure, which is consistent with the basic principles of the Hertz contact theory.

4.2. Design of Experiments: Second model

A second DOE was then realized with the previous influencing factors in a restricted domain study. The other factors values were kept in the optimum values calculated for the first model. The DOE was following a Doehlert matrix. The sampling per factor was 5 and induced 9 FEM simulations. The Variation values were chosen at ± 5 % of the Nominal values (Table 2). The RS follows the Equation 4 with 6 coefficients. Where N_i and $N_{i,j}$ were the response surface coefficients, Z_i were the normalized values of Q_i (Eq.2) and Q_i were the factor values (Table 2).

$$Y_2 = N_0 + N_1.Z_1 + N_2.Z_2 + N_{12}.Z_1.Z_2 + N_{11}.Z_1^2 + N_{22}.Z_2^2 \quad (4)$$

$$Zi = \frac{Qi - Nominal}{Variation} \quad (5)$$

Table 2
DOE parameters and results of the second model.

	Factor	Center	Variation	Optimum values
Q1	a_1	0.02045	0.00102	0.02047
Q2	c_1	0.09094	0.00455	0.09548

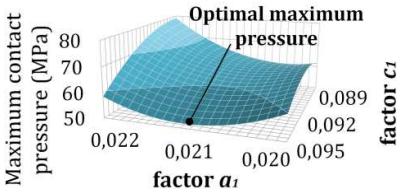

Figure 7. Surface response of the second model.

After calculation of the N_i and $N_{i,j}$ coefficients, the RS was drawn in Fig. 7. The optimal maximum contact pressure ($Y_{th\ min}$) was estimated at 51.8 MPa. The optimum factor values are shown in Optimum values column (Table 2). After the FEM calculation using these values, the maximum contact pressure was 55.8 MPa. This value was inside the error bar of the optimum maximum contact pressure estimated by the RS (45.3 to 58.2 MPa). The error bar was calculated with Equation 6. The value of k is 1.64 for error level of 95%.

$$Y_{th\ min} \pm k\sqrt{Var(Y_{th\ min})} \quad (6)$$

The bio-inspiration methodology was a first approach to enhance the contact pressure distribution for off-center load. The maximum contact pressure was 108 MPa for the bio-inspired bearing without optimization and 179 MPa for the cylindrical bush bearings. Then the DOE methodology was a second approach to enhance the contact pressure distribution. It has contributed to reduce the maximum contact pressure by a factor 2 (108 to 56 MPa). Thus, the combination of these two methodologies helps to reduce the maximum contact pressure by a factor 3 (179 to 56 MPa). The new design was integrated to the flight control system (Fig. 8). The outer ring was split in two for assembly feasibility. The inner shaft was made in one simple part. The bio-inspired bearing joint was angularly positioned so that there was no interruption in contact zones during joint rotation.

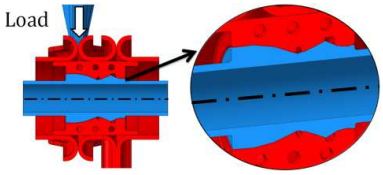

Figure 8. Integration of the bio-inspired bearing into the flight control system.

5. Conclusion and outlook

This study provides a new methodology to design and optimize a bio-inspired bearing for off-center load. Firstly, the bearing design was inspired by the cartilage shapes of lamb elbow. For that, the humerus and radius profiles were analyzed. Three potential contact zones were identified. Each of these contact zones was smoothed with polynomial of degree 2. The bio-inspired bearing was built by revolution of these smoothed profiles. Then the study has compared different clearance specifications via FEM computations in term of maximum contact pressure under off-center load. The normal clearance was found to be the best solution. Secondly, the bio-inspired bearing geometry was then optimized with 2 DOEs. The first DOE allowed to represent the solution design space to a large extent of parameters and found the factors the most influencing on pressure distribution. The second DOE surrogate model was defined with two most influencing parameters to predict the local optimum pressure distribution. The optimized bio-inspired bearing has showed a significant improvement in term of contact pressure compared with the cylindrical bush bearing. The contact pressure was reduced by a factor 3. A modification of a helicopter flight control system has been studied following this new bearing design.

Acknowledgments

This work was supported by Airbus Helicopters and Aix-Marseille University. The experimental devices were founded by: European Community, French Ministry of Research and Education and Aix-Marseille Conurbation Community.

References

[1] Marques, F., Isaac, F., Dourado, N., Flores, P, 2017, An enhanced formulation to model spatial revolute joints with radial and axial clearances, Mechanism and Machine Theory, 116, 123-144.
[2] Jang, J., Khonsari, M., 2015, On the Characteristics of Misaligned Journal Bearings, Lubricants 3(1), 27-53
[3] Youngua, C., Lu, J., 2011, Minimise joint clearance in rapid fabrication of non-assembly mechanisms, International Journal of Computer Integrated Manufacturing 24(8), 726-734.
[4] Byrne, G., Dimitrov, D., Monostori, L., Teti, R., Van Houten, F., Wertheim, R., 2018, Biologicalisation: Biological transformation in manufacturing, CIRP Journal of Manufacturing Science and Technology, 21, 1-32.
[5] Van der Linde, R., Caals, J., Menon, C., Verhoef, J., 2006, Biological Inspired Joints for Innovative Articulation Concepts, ESA Report.
[6] Poncery, B., Arroyave-Tobón, S., Picault, E., Linares, J.M., 2019, Effects of realistic sheep elbow kinematics in inverse dynamic simulation, PloS one, 14(3), e0213100.
[7] Picault, E., Mermoz, E., Thouveny, T., Linares, J.M., 2018, Smart pressure distribution estimation in biological joints for mechanical bio-inspired design, Annals of the CIRP 67(1), 153-156.
[8] Giannicola, G., Spinello, P., Scacchi, M., 2017, Cartilage thickness of distal humerus and its relationships with bone dimensions: magnetic resonance imaging bilateral study in healthy elbows, J. of shoulder and elbow surgery 26(5), e128-e136.
[9] Waide, D.V., Lawlor, G.J., Mccormack, BAO., 2000, The relationship between surface topography and contact in the elbow joint: development of a two-dimensional geometrical model in the coronal plane, Proceedings of the Institution of Mechanical Engineers, Part H: J. of Engineering in Medicine 214(4), 413-423.
[10] Germaneau, A., Peyruseigt, F., Mistou, S., 2008 Verification of a spherical plain bearing finite-element model using scattered light photo elasticity tests, Proceedings of the Institution of Mechanical Engineers, Part J: Journal of Engineering Tribology, 222(5), 647-656.